Chemistry of Metals and Alloys

Chem. Met. Alloys 3 (2010) 18-23
Ivan Franko National University of Lviv
www.chemetal-journal.org

The reciprocal system $CuGaS_2$+$CuInSe_2$⇆$CuGaSe_2$+$CuInS_2$

L.P. MARUSHKO[1*], Y.E. ROMANYUK[2], L.V. PISKACH[1], O.V. PARASYUK[1], I.D. OLEKSEYUK[1], S.V. VOLKOV[3], V.I. PEKHNYO[3]

[1] *Department of Inorganic and Physical Chemistry, Lesya Ukrainka Volyn National University, Voli Ave 13, 43025 Lutsk, Ukraine*
[2] *EMPA, Swiss Federal Laboratories for Materials Science and Technology, Überlandstrasse 129, CH 8600 Dübendorf, Switzerland*
[3] *V.I. Vernadskii Institute of General and Inorganic Chemistry of the Ukrainian National Academy of Sciences, Acad. Palladina Ave 32/34, 03680 Kyiv-142, Ukraine*
* *Corresponding author. Tel./fax: +380-3322-41007; e-mail: marushko777@mail.ru*

Received February 18, 2010; accepted June 29, 2010; available on-line November 5, 2010

Phase equilibria in the reciprocal system $CuGaS_2$+$CuInSe_2$⇆$CuGaSe_2$+$CuInS_2$ were investigated by differential thermal and X-ray phase analyses. The isothermal section of the system at 870 K was constructed. The region of existence of the α-solid solution range of the system components with chalcopyrite structure was determined. The vertical sections $CuGaS_2$–$CuGaSe_2$ and $CuGaS_2$–$CuInSe_2$ were constructed from DTA data.

Phase diagram / Isothermal section / Solid solution

Introduction

The finite quantity of fossil resources accelerates the development of renewable energy sources, of which solar energy is a promising front-runner. Increase of the efficiency and reduction of the cost of solar cells are researched both by trying to improve the production technology for cells based on already known materials and by searching for new materials. Alternatives to classic silicon in solar cells are $CuInSe_2$ (CIS) and its solid solutions. Among the primary challenges in the search for new materials the optimization of the composition of the solid solutions $CuInS_xSe_{2-x}$, $CuIn_xGa_{1-x}Se_2$ (CIGS), $CuIn_xGa_{1-x}S_ySe_{2-y}$ (CIGSSE) is attracting most interest [1-8].

The working element of CIS-based solar cells is the CIS/CdS heterojunction where *p*-type CIS is the absorption layer and *n*-type CdS is the buffer layer. The study of systems that combine the heterojunction components has interesting practical applications.

We have earlier investigated the ternary reciprocal systems $CuInS_2$+2CdSe⇆$CuInSe_2$+2CdS [9], $CuGaS_2$+2CdSe⇆$CuGaSe_2$+2CdS [10] and the ternary systems $CuGaS_2$–$CuInS_2$–2CdS [11], $CuGaSe_2$–$CuInSe_2$–2CdSe [12], which are the bounding sides of the quaternary reciprocal system CuIn, CuGa,Cd || S,Se (Fig. 1) that covers all variants of solid solutions of the ternary phases and the cadmium chalcogenides CdS and CdSe.

The $CuInS_2$+2CdSe⇆$CuInSe_2$+2CdS system features the existence of a γ-phase, which is a solid solution range of HT-modifications of $CuInS_2$ and $CuInSe_2$ with the sphalerite structure that is stabilized at the annealing temperatures (620 K and 870 K) by cadmium chalcogenides [9]. Physical properties of γ-solid solutions were studied on single crystals grown by the horizontal Bridgman method [13]. The crystals were photosensitive, primarily of *p*-type, with a carrier concentration of 10^{15}-10^{16} cm^{-3} and mobility 18 cm/(V·s); their bandgap energy ranges from 1.05 to 1.43 eV, thus suitable for the use in photovoltaic cells.

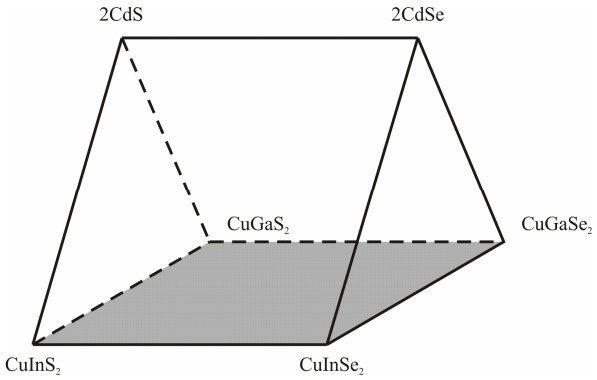

Fig. 1 Quaternary reciprocal system CuIn, CuGa,Cd || S,Se and the position of the reciprocal system $CuGaS_2$+$CuInSe_2$⇆$CuGaSe_2$+$CuInS_2$.

Minor γ-solid solution ranges have been found in the $CuGaS_2$+2CdSe⇆$CuGaSe_2$+2CdS system centered at the quaternary compound $CuCd_2GaSe_4$ [10] and in the $CuInS_2$–$CuGaS_2$–2CdS system [11].

The $CuGaSe_2$–$CuInSe_2$–2CdSe system exhibits a large range of γ-solid solutions based on the stabilized HT-$CuInSe_2$ and the $CuCd_2GaSe_4$ phases. Using the horizontal Bridgman method, 11 single crystals were grown from the γ-solid solution range along the '$CuCd_2InSe_4$'–$CuCd_2GaSe_4$ section [12].

The object of this paper is the reciprocal system $CuGaS_2$+$CuInSe_2$⇆$CuGaSe_2$+$CuInS_2$, which is also one of the bounding sides of the quaternary reciprocal system Cu,In, Cu,Ga,Cd || S,Se.

Literature data on the quasi-binary systems

The $CuGaS_2$–$CuGaSe_2$ system

The $CuGaS_2$–$CuGaSe_2$ system was studied in [14]. The $CuGaS_2$ thermogram features one effect at 1515 K, which corresponds to the melting point of the compound; the $CuGaSe_2$ thermogram shows two effects at 1320 and 1345 K. Two similar effects are observed for solid solutions near $CuGaSe_2$. The authors describe the thermal effect of $CuGaSe_2$ at 1320 K as an order-disorder polymorphous transition (cation-cation disordering) and ascribe the investigated phase diagram to Type I of Roozeboom's classification. The ternary compounds and their solid solutions crystallize in the chalcopyrite structure.

The $CuInS_2$–$CuInSe_2$ system

The $CuInS_2$–$CuInSe_2$ phase diagram was investigated in [9,15,16]. Two continuous solid solution series were found in the system, as well as a limited solid solution range of HT(2)-$CuInS_2$, which undergoes a metatectic decomposition (β→L+γ) at 1315 K. The coordinates of the invariant point are 31 mol.% $CuInSe_2$ and 1315 K.

The $CuGaS_2$–$CuInS_2$ system

The $CuGaS_2$–$CuInS_2$ phase diagram was investigated in [17,18]. Our report [18] established that the $CuGaS_2$–$CuInS_2$ diagram is of peritectic type with two peritectic points: 45 mol.% $CuGaS_2$, 1426 K and 68 mol.% $CuGaS_2$, 1451 K. The system features a continuous α-solid solution series and two limited β- and γ-solid solution ranges, based on the HT(1) and HT(2) modifications of $CuInS_2$, respectively.

The $CuGaSe_2$–$CuInSe_2$ system

The $CuGaSe_2$–$CuInSe_2$ system was investigated in [12,22]. The phase diagram [22] was ascribed to Type I of Roozeboom's classification. The thermograms of the ternary compounds feature two thermal effects, at 1318 and 1361 K for $CuGaSe_2$, and at 1083 and 1259 K for $CuInSe_2$. The phase transitions at 1318 and 1083 K were interpreted as cation-cation disordering. Similar phase transitions characterize the solid solution $CuGa_xIn_{1-x}Se_2$ in the entire concentration range. However, the phase diagram is inconsistent with the fact that $CuGaSe_2$ forms in the Cu_2Se–Ga_2Se_3 system by a peritectic reaction [19-21]. This was the reason for the re-investigation of the system. Our diagram [12] agrees well with the version in [22] at low temperatures, but features additional fields at near-liquidus temperatures in the $CuGaSe_2$-rich region, which are caused by the incongruent formation of copper selenogallate.

Single crystals of the solid solution $CuGa_xIn_{1-x}Se_2$ obtained in [23] had the chalcopyrite structure and *p*-type conductivity.

Experimental

A total of 90 alloys were synthesized for the investigation of the phase equilibria in the reciprocal system $CuGaS_2$+$CuInSe_2$⇆$CuGaSe_2$+$CuInS_2$; their compositions are presented in Fig. 2. The alloys were synthesized from the elements (Cu, Ga, In, S, Se) with a content of the main element of at least 99.99 wt.%. The calculated amounts were placed into quartz ampoules that were evacuated to the residual pressure 10^{-2} Pa and soldered. The synthesis was performed in two stages. At the first stage the ampoules with the batches were heated in the flame of an oxygen-gas burner with visual control of the process (to complete bonding of sulfur). At the second stage the ampoules were heated in a single-zone shaft-type furnace at the rate of 50 K/h to a maximum synthesis temperature of 1470 K. After 2-3 h exposure the ampoules were slowly cooled at the rate of 10 K/h to 870 K. The samples were annealed at this temperature for 1500 h, followed by quenching into cold water. This process resulted in compact dark-grey polycrystalline ingots.

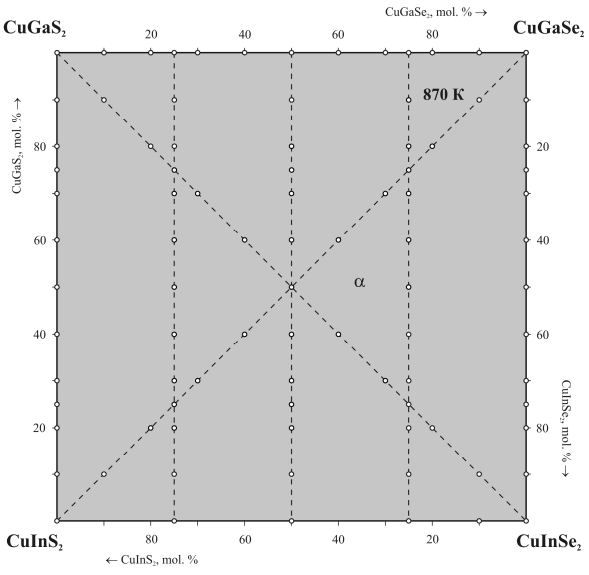

Fig. 2 Chemical composition of the alloys and the isothermal section of the reciprocal system $CuGaS_2$+$CuInSe_2$⇆$CuGaSe_2$+$CuInS_2$ at 870 K.

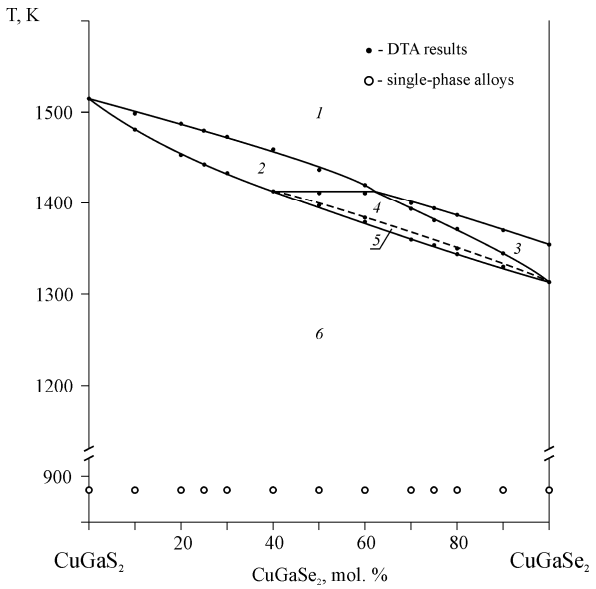

Fig. 3 Vertical section $CuGaS_2$–$CuGaSe_2$: 1 – L; 2 – L+α; 3 – L+γ'; 4 – L+α+γ'; 5 – α+γ'; 6 – α.

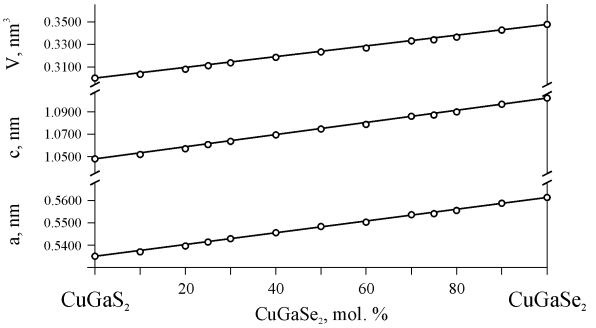

Fig. 4 Variation of the unit cell parameters of the alloys of the $CuGaS_2$–$CuGaSe_2$ section at 870 K.

The obtained alloys were investigated by differential thermal analysis (Paulik-Paulik-Erdey derivatograph, Pt/Pt-Rh thermocouple) and XRD (DRON 4-13 diffractometer, CuK_α radiation). The lattice parameters were computed using the PDWin-2 software package.

Results and discussion

The isothermal section of the reciprocal system $CuGaS_2$+$CuInSe_2$⇆$CuGaSe_2$+$CuInS_2$ at 870 K

The isothermal section of the reciprocal system $CuGaS_2$+$CuInSe_2$⇆$CuGaSe_2$+$CuInS_2$ at 870 K, constructed from the results of the X-ray phase analysis of the alloys, is presented in Fig. 2. At this temperature the system exists as an α-solid solution of $CuGaS_2$, $CuGaSe_2$, HT-$CuInS_2$ and HT-$CuInSe_2$ with the chalcopyrite structure that occupies the entire concentration square.

The vertical section $CuGaS_2$–$CuGaSe_2$

The $CuGaS_2$–$CuGaSe_2$ system is one of the sides of the reciprocal system. The phase diagram is non-quasi-binary above the solidus due to the incongruent melting of the $CuGaSe_2$ compound. The vertical section is presented in Fig. 3. The liquidus consists of two lines that belong to the fields of primary crystallization of γ'-phase, which participates in the peritectic process of formation of $CuGaSe_2$ (the homogeneity region of the γ'-phase is localized in the Cu_2Se–Ga_2Se_3 section) and of the α-phase, which is the solid solution of $CuGaSe_2$ and $CuGaS_2$. The fields of primary crystallization are separated by the three-phase field L+α+γ'. XRD data show that all alloys annealed at 870 K are single-phase and crystallize in the tetragonal chalcopyrite structure (Fig. 4), which agrees well with the results of [14].

The $CuGaS_2$–$CuInSe_2$, $CuGaSe_2$–$CuInS_2$ sections

The vertical section $CuGaS_2$–$CuInSe_2$ (Fig. 5) is a diagonal section of the phase diagram of the reciprocal system $CuGaS_2$+$CuInSe_2$⇆$CuGaSe_2$+$CuInS_2$. The section liquidus consists of the curves of primary crystallization of the α- and γ-solid solutions. The section is non-quasi-binary below the liquidus (it crosses the monovariant line that separates the fields of primary crystallization of the α- and γ-solid solutions). γ-solid solutions of HT-$CuInSe_2$ exist only at high temperatures and decompose upon cooling. The thermograms of selected alloys are presented in Fig. 6.

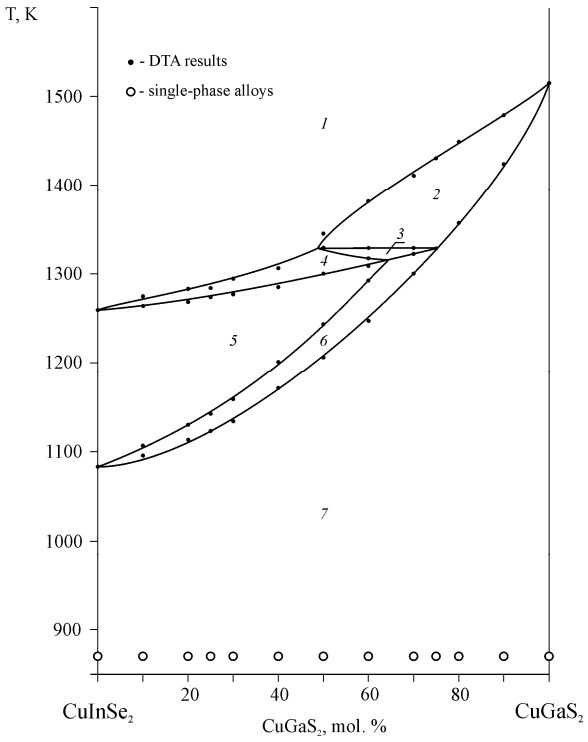

Fig. 5 Vertical section $CuGaS_2$–$CuInSe_2$: 1 – L; 2 – L+α; 3 – L+α+γ; 4 – L+γ; 5 – γ; 6 – α+γ; 7 – α.

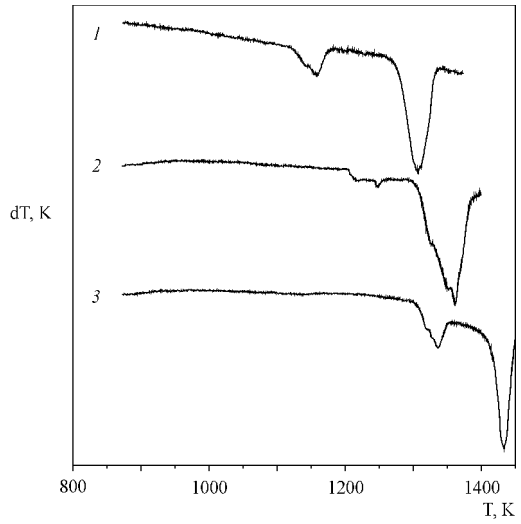

Fig. 6 Thermograms of alloys at the $CuGaS_2$–$CuInSe_2$ section (mol.% $CuInSe_2$): 1 – 25; 2 – 50; 3 – 70.

All alloys of the $CuGaS_2$–$CuInSe_2$ section are single-phase at the annealing temperature and crystallize in the chalcopyrite structure of the α-solid solutions (Fig. 7). The change of the unit cell parameters with composition follows Vegard's rule (Fig. 8).

The other diagonal of the phase diagram of the reciprocal system $CuGaS_2$+$CuInSe_2$⇆$CuGaSe_2$+$CuInS_2$ is the $CuGaSe_2$–$CuInS_2$ section. All alloys of this section are also single-phase (Figs. 9,10).

The 'CuGaS$_{1.5}$Se$_{0.5}$'–'CuInS$_{1.5}$Se$_{0.5}$', 'CuGaSSe'–'CuInSSe' and 'CuGaS$_{0.5}$Se$_{1.5}$'–'CuInS$_{0.5}$Se$_{1.5}$' sections

According to XRD data, all the alloys from the 'CuGaS$_{1.5}$Se$_{0.5}$'–'CuInS$_{1.5}$Se$_{0.5}$', 'CuGaSSe'–'CuInSSe' and 'CuGaS$_{0.5}$Se$_{1.5}$'–'CuInS$_{0.5}$Se$_{1.5}$' sections are single-phase. The change of the unit cell parameters along these sections is plotted in Figs. 11-13.

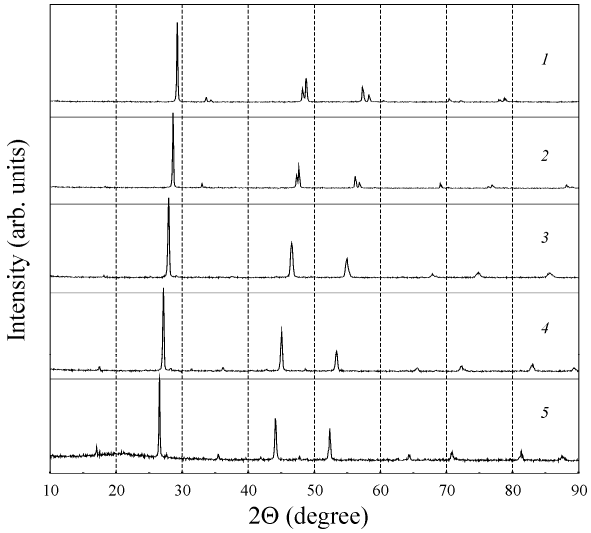

Fig. 7 Diffraction patterns of alloys of the $CuGaS_2$–$CuInSe_2$ section (mol.% $CuInSe_2$): 1 – 0; 2 – 20; 3 – 50; 4 – 80; 5 – 100.

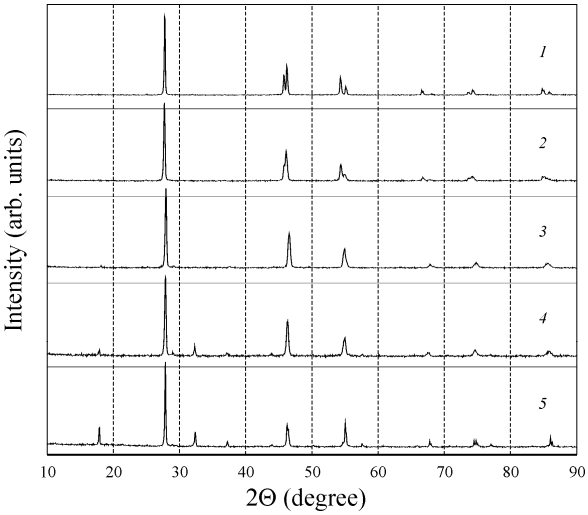

Fig. 9 Diffraction patterns of alloys of the $CuGaSe_2$–$CuInS_2$ section (mol.% $CuInS_2$): 1 – 0; 2 – 20; 3 – 50; 4 – 80; 5 – 100.

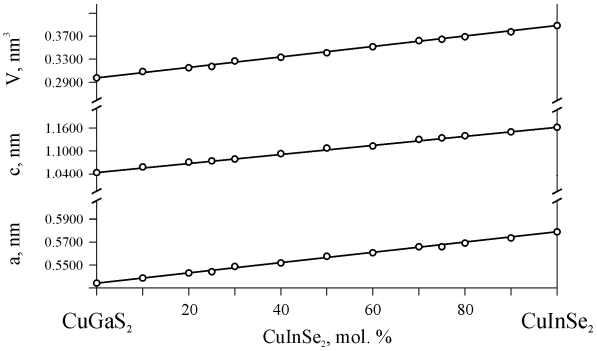

Fig. 8 Variation of the unit cell parameters of the alloys of the $CuGaS_2$–$CuInSe_2$ section at 870 K.

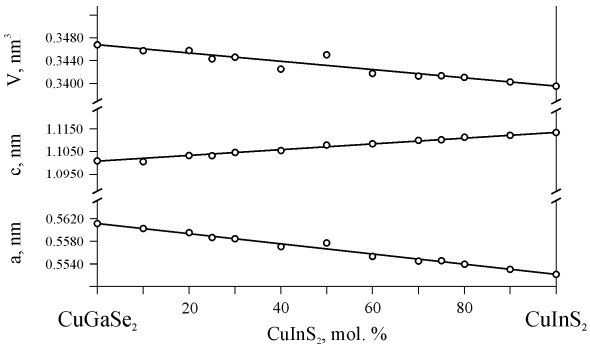

Fig. 10 Variation of the unit cell parameters of the alloys of the $CuGaSe_2$–$CuInS_2$ section at 870 K.

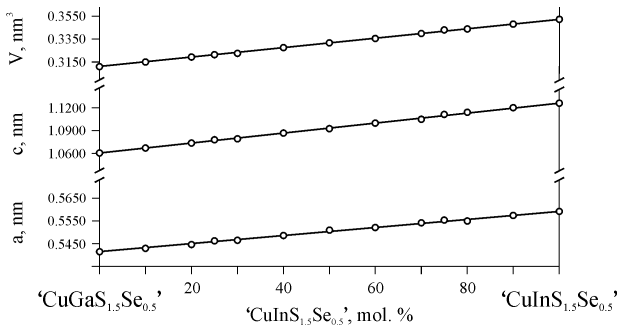

Fig. 11 Variation of the unit cell parameters of the alloys of the '$CuGaS_{1.5}Se_{0.5}$'–'$CuInS_{1.5}Se_{0.5}$' section at 870 K.

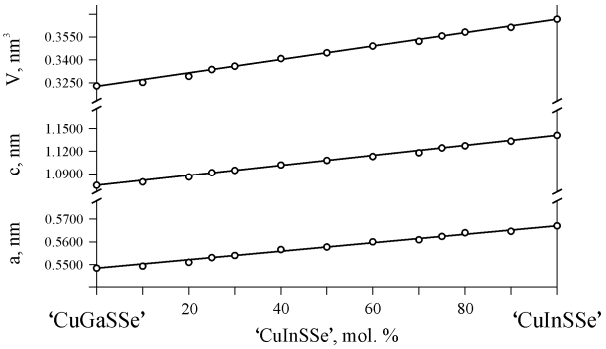

Fig. 12 Variation of the unit cell parameters of the alloys of the 'CuGaSSe'–'CuInSSe' section at 870 K.

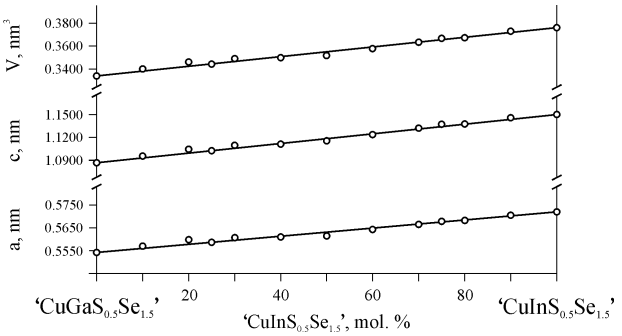

Fig. 13 Variation of the unit cell parameters of the alloys of the '$CuGaS_{0.5}Se_{1.5}$'–'$CuInS_{0.5}Se_{1.5}$' section at 870 K.

Conclusions

The reciprocal system $CuGaS_2$+$CuInSe_2$⇆ $CuGaSe_2$+$CuInS_2$ was investigated by DTA and XRD methods. At 870 K the system is a continuous solid solution series of its components with the chalcopyrite structure. The vertical sections $CuGaS_2$–$CuGaSe_2$ and $CuGaS_2$–$CuInSe_2$ were constructed. As $CuInSe_2$-based solid solutions are widely used in solar cells, a thorough study of the physical properties of the solid solutions that exist in the reciprocal system $CuGaS_2$+$CuInSe_2$⇆$CuGaSe_2$+$CuInS_2$ is necessary.

References

[1] A. Goetzberger, C. Hebling, H.-W. Schock, *Mater. Sci. Eng.* 40 (2003) 1.
[2] R.W. Miles, K.M. Hynes, I. Forbes, *Prog. Cryst. Growth Charact. Mater.* 51 (2005) 1.
[3] K. Ramanathan, F.S. Hasoon, S. Smith, D.L. Young, M.A. Contreras, P.K. Johnson, A.O. Pudov, J.R. Sites, *J. Phys. Chem. Solids* 64 (2003) 1495.
[4] R.W. Miles, K.T. Ramakrishna Reddy, I. Forbes, *J. Cryst. Growth* 198–199 (1999) 316.
[5] T. Walter, A. Content, K.O. Velthaus, H.W. Schock, *Sol. Energy Mater. Sol. Cells* 26 (1992) 357.
[6] J. Djordjevic, C. Pietzker, R. Scheer, *J. Phys. Chem. Solids* 64 (2003) 1843.
[7] V. Probst, J. Palm, S. Visbeck, T. Niesen, R. Tölle, A. Lerchenberger, M. Wendl, H. Vogt, H. Calwer, W. Stetter, F. Karg, *Sol. Energy Mater. Sol. Cells* 90 (2006) 3115.
[8] Th. Glatzel, H. Steigert, S. Sadewasser, R. Klenk, M. Ch. Lux-Steiner, *Thin Solid Films* 480-481 (2005) 177.
[9] O.V. Parasyuk, I.D. Olekseyuk, V.I. Zaremba, O.A. Dzham, Z.V. Lavrynyuk, L.V. Piskach, O.G. Yanko, S.V. Volkov, V.I. Pekhnyo, *J. Solid State Chem.* 179 (2006) 2998.
[10] L.V. Piskach, Z.V. Lavrynyuk, O.V. Parasyuk, O.F. Zmiy, E.M. Kadykalo, V.I. Pekhnyo, S.V. Volkov, *Nauk. Visn. Volyn. Nats. Univ.* 16 (2008) 47.
[11] L.P. Marushko, L.V. Piskach, Y.E. Romanyuk, O.V. Parasyuk, I.D. Olekseyuk, S.V. Volkov, V.I. Pekhnyo, *J. Alloys Compd.* 492 (2010) 184.
[12] L.P. Marushko, Y.E. Romanyuk, L.V. Piskach, O.V. Parasyuk, I.D. Olekseyuk, S.V. Volkov, V.I. Pekhnyo, *J. Alloys Compd.* 505 (2010) 101.
[13] Y.E. Romanyuk, K.M. Yu, W. Walukiewicz, Z.V. Lavrynyuk, V.I. Pekhnyo, O.V. Parasyuk, *Sol. Energy Mater. Sol. Cells* 92 (2008) 1495.
[14] I.V. Bodnar, A.P. Bologa, *Neorg. Mater.* 18 (1982) 1257.
[15] E.N. Kholina, V.B. Ufimtsev, A.S. Timoshyn, *Neorg. Mater.* 15 (1979) 1918.
[16] I.V. Bodnar, A.P. Bologa, B.V. Korzun, *Krist. Tech.* 15 (1980) 1285.

[17] I.V. Bodnar, *Neorg. Mater.* 17 (1981) 583.
[18] L.P. Marushko, L.V. Piskach, O.V. Parasyuk, V.I. Pekhnyo, *Nauk. Visn. Volyn. Nats. Univ.* 13 (2007) 3.
[19] L.S. Palatnik, Ye.K. Belova, *Neorg. Mater.* 3 (1967) 967.
[20] L.S. Palatnik, Ye.K. Belova, *Neorg. Mater.* 3 (1967) 2194.
[21] J.C. Mikkelsen, *J. Electron. Mater.* 10 (1981) 541.
[22] I.V. Bodnar, A.P. Bologa, *Cryst. Res. Technol.* 17 (1982) 339.
[23] K. Yoshino, H. Yokoyama, K. Meada, T. Ikari, *J. Cryst. Growth* 211 (2000) 476.